Hepatocytes convert to a fibroblastoid phenotype through the cooperation of TGF-β1 and Ha-Ras: steps towards invasiveness

Josef Gotzmann[1], Heidemarie Huber[1], Christiane Thallinger[2], Markus Wolschek[2], Burkhard Jansen[2], Rolf Schulte-Hermann[1], Hartmut Beug[3] and Wolfgang Mikulits[1,*]

[1]Institute of Cancer Research, University of Vienna, Borschke-Gasse 8a, A-1090 Vienna
[2]Department of Clinical Pharmacology, Section of Experimental Oncology, Vienna General Hospital, Währinger Gürtel 18-20, A-1090 Vienna
[3]Research Institute of Molecular Pathology, Dr Bohr-Gasse 7, A-1030 Vienna, Austria
*Author for correspondence (e-mail: wolfgang.mikulits@univie.ac.at)

Accepted 6 December 2001
Journal of Cell Science 115, 1189-1202 (2002) © The Company of Biologists Ltd

Summary

In hepatocarcinogenesis, it is an open question whether transforming growth factor (TGF)-β1 provides a tumor-suppressive or a tumor-promoting role. To address this question, we employed immortalized murine hepatocytes, which display a high degree of differentiation and, expectedly, arrest in the G1 phase under exposure to TGF-β1. These hepatocytes maintain epithelial polarization upon expression of oncogenic Ha-Ras. However, Ras-transformed hepatocytes rapidly convert to a spindle-shaped, fibroblastoid morphology upon treatment with TGF-β1, which no longer inhibits proliferation. This epithelial to fibroblastoid conversion (EFC) is accompanied by disruption of intercellular contacts and remodeling of the cytoskeletal framework. Fibroblastoid derivatives form elongated branching cords in collagen gels and grow to severely vascularized tumors in vivo, indicating their increased malignancy and even invasive phenotype. Additionally, fibroblastoid cells secrete strongly enhanced levels of TGF-β1, suggesting an autocrine regulation of TGF-β signaling. Expression profiling further revealed that the loss of the adhesion component E-cadherin correlates with the upregulation of its transcriptional repressor Snail in fibroblastoid cells. Moreover, the phosphoinositide 3-OH (PI3) kinase pathway was required for the maintenance of EFC, as inhibition of PI3 kinase reverted fibroblastoid cells to an epithelial-like phenotype. Taken together, these data indicate a dual role of TGF-β1 in hepatocytes: it induces proliferation arrest but provides a crucial function in promoting late malignant events in collaboration with activated Ha-Ras.

Key words: Hepatocytes, Ha-Ras, TGF-β1, Epithelial polarity, Invasive growth

Introduction

Carcinomas account for most tumors and arise from the aberrant control of proliferation and the preceding dedifferentiation of epithelial cells. Upon progression of epithelial tumors to more malignant stages, carcinoma cells lose specific intercellular contacts, which are required to maintain the regular turnover and typical architecture of epithelial structures in the adult. The dissociation of cell-to-cell contacts and the concomitant acquisition of a fibroblastoid morphology is accompanied by the rearrangement of the cytoskeleton and the secretion of extracellular matrix proteins, which facilitates the adoption of a migratory and invasive phenotype at later steps of carcinogenesis (Birchmeier et al., 1995; Hay, 1990). A similar morphogenetic process, referred to as epithelial to mesenchymal (fibroblastoid) transition, occurs under precise spatio-temporal control during embryonic development, and it is conceivable that mechanisms contributing to this process might be reactivated upon tumorigenesis. Several cell-autonomous events, as well as external stimuli, have been reported to be involved in the establishment of aggressive undifferentiated types of carcinomas (Boyer et al., 2000).

The constitutive activation of receptor tyrosine kinases and their intracellular signaling components is a frequent event contributing to initiation and maintenance of malignant transformation (Hanahan and Weinberg, 2000). Among these, Ras represents a key signal transducer that integrates signals from many receptors (Rommel and Hafen, 1998; Shields et al., 2000). Depending on the activation of effectors downstream of Ras, specific pathways are able to promote various cellular phenotypes (Downward, 1998; McCormick, 1999). The multiple downstream effectors of Ras include (i) Raf, which activates the Erk/MAP kinase pathway (considered to have implications in proliferation, differentiation and apoptosis), (ii) the lipid kinase phosphoinositide 3-OH (PI3)3 kinase, which stimulates PKB/Akt kinase to provide signals for cell survival, and (iii) the small GTPases Rac and Rho, which are both able to affect cell motility through modulation of the cytoskeleton (Schmitz et al., 2000).

Murine liver carcinomas express activated Ha-Ras in 70% of cases, supporting the idea that Ha-Ras plays a key role in the induction of hepatocellular carcinogenesis (Reynolds et al., 1986; Reynolds et al., 1987; Saitoh et al., 1990; Strom and Faust, 1990; Fausto and Webber, 1993). Indeed, studies of liver

growth regulation and carcinogenesis employing transgenic mice showed that the overexpression and mutation of Ha-Ras results in rapid formation of adenomas and carcinomas (Sandgren et al., 1989). Although mutational activation of Ras proteins occurs in human liver tumors with an incidence of only about 5% (Bos, 1989), receptor-mediated hyperactivation of Ras-dependent signal transduction pathways is a frequent event in human carcinogenesis (Clark and Der, 1995; Graziani et al., 1993; Jo et al., 2000; Thiery and Chopin, 1999).

External stimuli provided by specific growth factors regulate epithelial cell differentiation and plasticity through binding to their cognate receptors. Among these, the transforming growth factor (TGF)-β family of cytokines is particularly important in controlling proliferation, apoptosis and morphogenesis of epithelial cells. Particularly, it has been found that TGF-β acts as a potent growth inhibitor of epithelial cell proliferation through its ability to dysregulate inhibitors of cyclin dependent kinases, which cause arrest in the G1 phase of the cell cycle (Reynisdottir et al., 1995). To accomplish its regulatory role, TGF-β transduces signals across the plasma membrane through heteromeric complexes of type I and II of TGF-β receptors (TβR-I and II; Massague, 1990). Ligand-activated TβR-II phosphorylates TβR-I, which induces intracellular signaling through the modulation and transactivation of Smads (Massague and Chen, 2000; Ten-Dijke et al., 2000). Complexes of regulatory Smad2 or Smad3 with the shared adapter molecule Smad4 translocate into the nucleus and associate with sequence-specific DNA-binding proteins to modulate transcription of specific target genes such as, for example, the extracellular matrix molecules fibronectin and plasminogen activator inhibitor type 1 (PAI-1). During the past years, however, evidence also accumulated that the loss of sensitivity to the growth inhibitory effect of TGF-β1 might play an important role in the progression of a variety of tumors (Cui et al., 1996; Markowitz et al., 1995; Portella et al., 1998). Studies on keratinocyte, mammary and prostate epithelial carcinogenesis models showed a synergistic cooperation of TGF-β and Ras to induce progression to undifferentiated, invasive tumors (Iglesias et al., 2000; Oft et al., 1996; Oft et al., 1998; Park et al., 2000).

Hepatocytes of the normal adult liver express undetectable levels of TGF-β1 but they respond to TGF-β1 produced by non-parenchymal liver cells through inhibition of DNA synthesis and induction of apoptosis (Oberhammer et al., 1991; Oberhammer et al., 1992; Rossmanith and Schulte-Hermann, 2001). Accordingly, TGF-β1 has been suggested to control homeostasis of liver mass in vivo through its contribution to the termination of hepatic proliferation upon liver regeneration and elimination of surplus hepatic cells during adaptive liver growth (Rossmanith and Schulte-Hermann, 2001; Fausto, 2000). Owing to the ability of hepatocytes to inhibit proliferation and to stimulate cell death, a tumor-suppressive activity has been assigned to TGF-β1 (Michalopoulos and DeFrances, 1997). In contrast, the overexpression of TGF-β1 and the concomitant resistance of hepatocytes to growth inhibition was frequently observed in hepatocellular carcinomas (HCC) (Bedossa et al., 1995; Factor et al., 1997; Grasl-Kraupp et al., 1998; Huggett et al., 1991; Ito et al., 1991; Zhao and Zimmermann, 1998). These findings supported the idea that TGF-β1 correlates with a tumor-promoting role and thus opened a controversial discussion on the functional implications of TGF-β1 upon liver tumorigenesis.

In the current study, we focused on the putative dual function of TGF-β1 in hepatocytes by analyzing the potential of TGF-β1 to induce growth inhibition as well as to promote malignant transformation. We first present evidence that TGF-β1, while arresting parental immortalized hepatocytes in the G1 phase, induces a hepatocellular epithelial to fibroblastoid conversion (EFC) in cooperation with activated Ha-Ras. The switch to a spindle-shaped, depolarized morphology leads to the establishment of a highly malignant and invasive phenotype, which secretes TGF-β1 in an autocrine fashion. Finally, we show that inhibition of PI3 kinase is sufficient to interfere with the TGF-β1-mediated invasive phenotype, as fibroblastoid cells revert to an epithelial-like morphology.

Materials and Methods

Cell culture and retroviral transfection

Immortalized Met murine hepatocytes (MMH-D3) were cultured in RPMI 1640 supplemented with 10% fetal calf serum (FCS), 40 ng/ml recombinant human TGF-α (Sigma, St. Louis, USA), 30 ng/ml recombinant human insulin-like growth factor II (IGF-II, Sigma, St. Louis, USA), 1.4 nM insulin (Sigma, St. Louis, USA) and antibiotics, as described recently (Amicone et al., 1997). The mouse fibroblast cell line Swiss 3T3 and human lung carcinoma cells A549 (American Type Culture Collection CCL-185) were grown in Dulbecco's modification of Eagles' Medium containing 10% FCS and antibiotics.

MMH-R cells were generated by retroviral transmission of parental MMH-D3 cells with a vector bicistronically expressing constitutive active v-Ha-Ras (Oft et al., 1996; Redmond et al., 1988) and green fluorescent protein (GFP). Selection and propagation of a v-Ha-Ras/GFP-positive cell population was performed by subculturing at a ratio of 1:3 twice a week in medium plus growth factors as described for MMH-D3 cells. Fibroblastoid-converted MMH-RT cells were cultured in RPMI 1640 supplemented with 15% FCS, 1 ng/ml recombinant human TGF-β1 (R&D Systems, Minneapolis, USA) and antibiotics. All cells were kept at 37°C and 5% CO_2 and routinely screened for the absence of mycoplasma.

The inhibitors PD98059 (Alexis Corporation, San Diego, USA), Wortmannin (Alexis Corporation, San Diego, USA), UO126 (Promega, Madison, USA) and LY294.002 (Alexis Corporation, San Diego, USA) were added to the culture medium at concentrations indicated in the text.

Proliferation kinetics

5×10^5 cells were seeded in triplicate on petri dishes with medium containing a combination of growth factors (as indicated in the text). Culture medium was replaced every second day. The number of cells in the corresponding cell populations was determined periodically in a multichannel cell analyzer (CASY; Schärfe Systems, Reutlingen, Germany). Cumulative cell numbers were calculated from the cell counts plus dilution factors.

Flow cytometry

The analysis of cellular DNA content was performed with a flow cytometer (FACSCalibur, Becton Dickinson, Franklin Lakes, USA). Prior to the cytofluorometric measurement, about 5×10^5 cells were washed with phosphate buffered saline (PBS), fixed in 70% ethanol, washed again with PBS and treated with 100 μg RNAse A/50 μg propidium iodide per ml for 10 minutes to stain cellular DNA. The percentage of cells in the various cell cycle positions was calculated using a software package from the same manufacturer.

Immunofluorescence

Cells grown on filters (Falcon 353090, Becton Dickinson, Franklin Lakes, USA) and frozen sections of excised tumor tissues were fixed in 3% formaldehyde/PBS for 20 minutes at room temperature (alternative fixation in acetone/methanol 1:2 at –20°C for 5 minutes) and permeabilized in 0.5% Triton X-100/PBS for 5 minutes. Subsequently, filters were cut into pieces and each part was incubated with the primary antibody diluted in PBS/0.2% gelatine for 60 minutes at room temperature. Dilutions of primary antibodies were as follows: anti-E-cadherin (Transduction Laboratories (TL), Lexington, UK), 1:100; anti-N-cadherin (TL), 1:150; anti-β-catenin (TL), 1:125; $p120^{ctn}$ (TL), 1:200; anti-Smad2 (TL), 1:250; anti-ZO-1 (Zymed Laboratories, South San Francisco, USA), 1:75; anti-desmoplakin (Parrish et al., 1987), 1:200; Phalloidin-TexasRed (Molecular Probes, Leiden, The Netherlands), 1:75; anti-von Willebrand Factor (Sigma, St.Louis, USA), 1:500. Cye-dye-conjugated secondary antibodies (Jackson Laboratories, West-Grove, USA) were applied for 30 minutes at room temperature at a dilution of 1:150 in PBS/0.2% gelatine. Single optical section images were generated by computer-driven data acquisition and optimized by photomultiplier modulation. Cells were imaged with the TCS-SP confocal microscope (Leica, Heidelberg, Germany) using a 60×1.3 NA lens objective with immersion oil (n=1.518). Conventional microscopy of cells was performed on a Nikon Eclipse TE300 inverted light microscope (Nikon Corporation, Tokyo, Japan) equipped for fluorescence image acquisition. For better illustration and for reasons of enhanced contrast, some microscopic pictures were colored green or red, respectively, in silico, although the cells themselves fluoresce green because of GFP expression.

Immunoblotting

Cellular extracts were prepared by swelling cells on ice for 5 minutes in hypotonic buffer (10 mM HEPES/KOH, pH 7.5, 5 mM KCl, 1.5 mM $MgCl_2$, 1 mM EDTA, 1 mM EGTA, 2 mM DTT supplemented with a proteinase inhibitor cocktail; 400 µl buffer per 10^7 cells). Cells were disrupted by pushing through a syringe equipped with a 27 gauge needle, and complete lysis was confirmed by microscopic inspection. The homogenate was supplied with 50 µg/ml DNase, 20 µg/ml RNAse A and 0.5% Nonidet-P40 and incubated at room temperature for 15 minutes. The lysate was supplemented with 2×SDS-PAGE sample buffer (40 mM Tris-HCl, pH 6.8, 2% SDS, 2% β-mercaptoethanol, 20% sucrose, 40 mM DTT, 0.5% bromophenol-blue) and boiled at 95°C for 5 minutes. All lysates were normalized to a protein yield of 1×10^5 cells. SDS-PAGE and immunoblotting was performed essentially as described by Gotzmann et al. (Gotzmann et al., 1997), except that the immunological detection of proteins was performed with the SuperSignal detection system (Pierce Chemical Company, Rockford, USA). The following primary antibodies diluted in TBS were used: anti-E-cadherin (Transduction Laboratories (TL), Lexington, UK), 1:3.000; anti-N-cadherin (TL), 1:1.500; anti-β-catenin (TL), 1:1.000; anti-ZO-1 (Zymed Laboratories, South San Francisco, USA), 1:1.500; anti-Ras (DAKO, Carpinteria, USA), 1:250; anti-desmoplakin (Parrish et al., 1987), 1:25; anti-phosphoSmad2 (Upstate Biotechnology, Waltham, USA), 1:150; GAPDH, 1:5000 (Chemicon, Temecula, USA). Secondary antibodies (BioRad, Richmond, USA) were used at dilutions of 1:2.000.

Transepithelial electrical resistance (TER)

For measuring TER (Oft et al., 1996), cells were plated on polycarbonate filters (Falcon 353090, Becton Dickinson, Franklin Lakes, USA) with a pore size of 0.4 µm at 70-80% confluency. The growth medium was changed every second day and the resistance determined with a volt-ohm meter after 7 days of growth at high density. Measurements were performed in triplicate and assays were repeated twice. All TER values were normalized to background values (filter in PBS only).

Colony formation in soft agar

To test the ability of cells to grow independently of anchorage in semi-

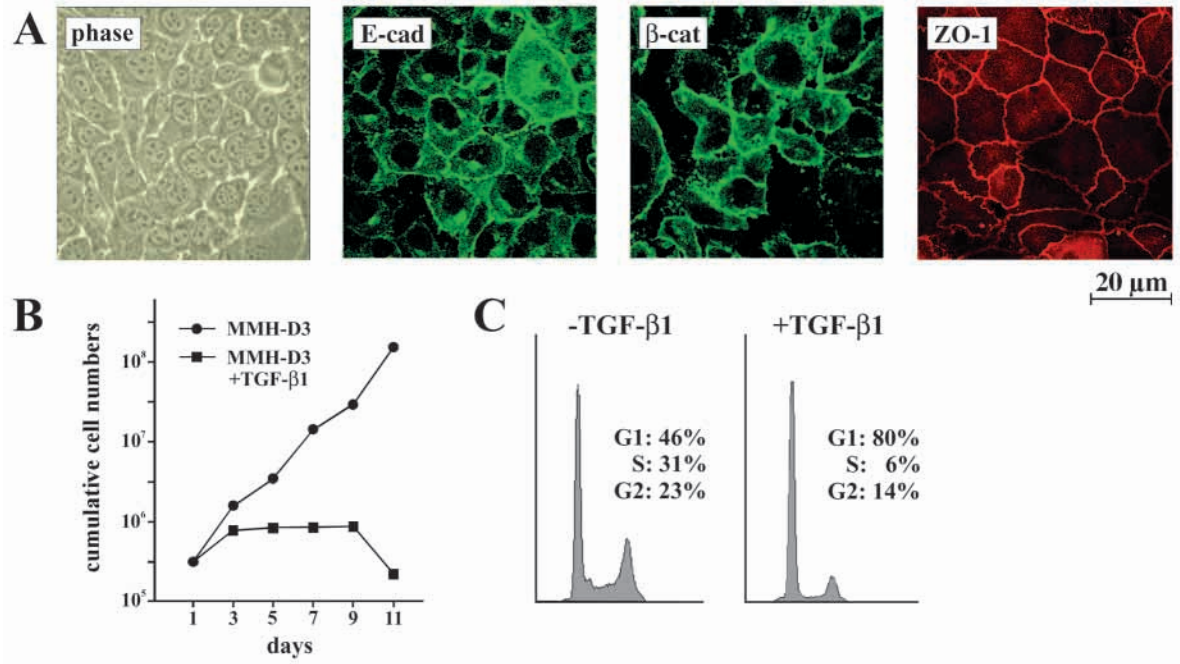

Fig. 1. MMH-D3 cells display a polarized phenotype and respond to the growth inhibitory function of TGF-β1. (A) Phase contrast and confocal immunofluorescence microscopy of parental MMH-D3 cells stained with the adherens junction markers E-cadherin and β-catenin and the tight junction marker ZO-1. (B) Proliferation kinetics of MMH-D3 cells (circles) versus MMH-D3 supplemented with 5 ng/ml TGF-β1 (squares). (C) Flow cytometry determining the cell cycle distribution of MMH-D3 cells versus MMH-D3 at day 5 of TGF-β1 (5 ng/ml) treatment.

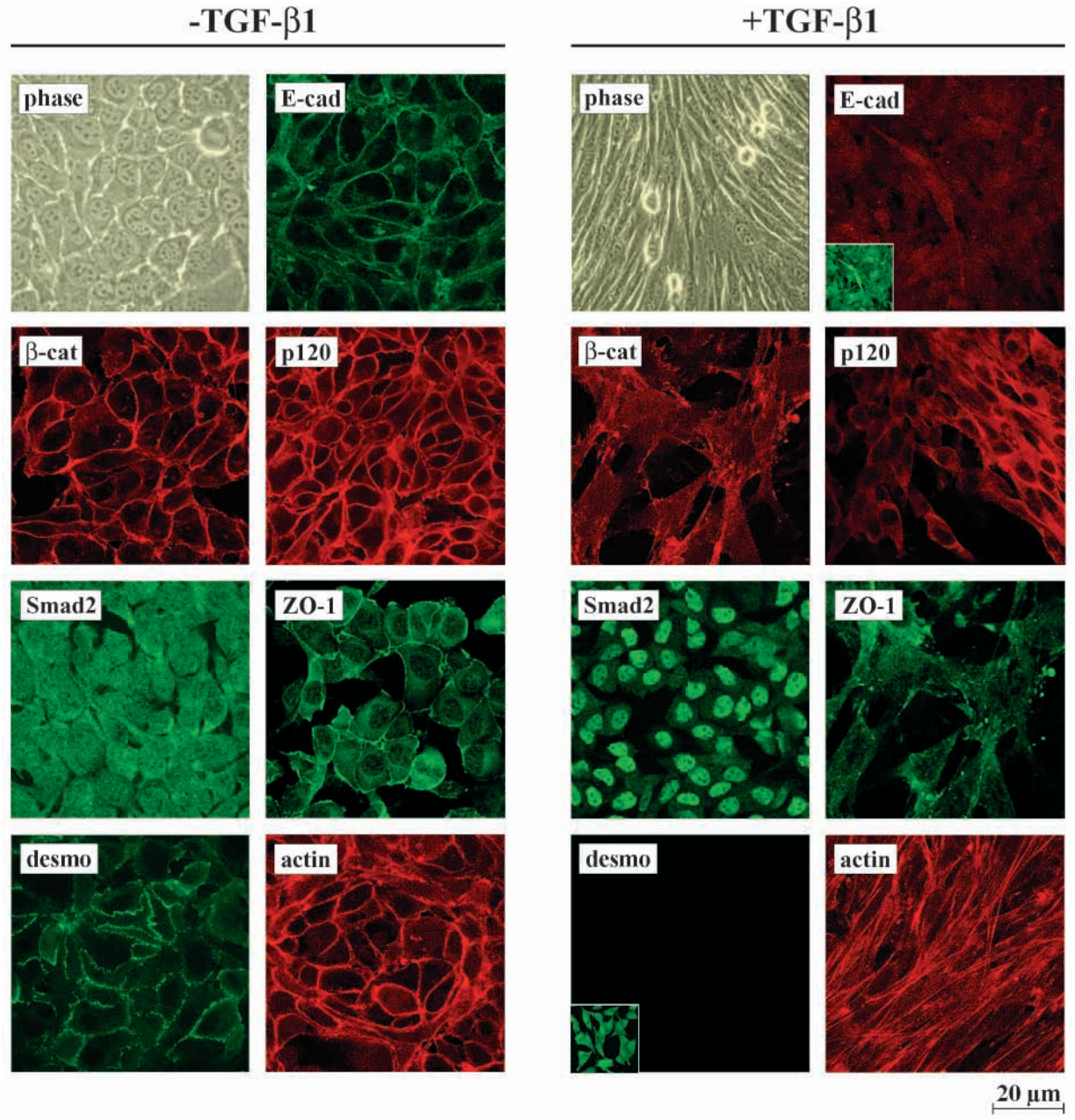

Fig. 2. TGF-β1 triggers an epithelial to fibroblastoid conversion of MMH-R cells expressing constitutive active Ha-Ras. Left panel (–TGF-β1): MMH-R cells show a polarized epithelial phenotype as analyzed by phase contrast and confocal immunofluorescence microscopy. Right panel (+TGF-β1): Epithelial MMH-R cells treated with 5 ng/ml TGF-β1 undergo a conversion to a spindle-shaped fibroblastoid phenotype. The resulting depolarized MMH-RT cell type was processed for microscopical inspection. Exceptionally, cells were stained for Smad2 30 minutes after TGF-β1 induction. Insets in panels of undetectable E-cadherin and desmoplakin staining indicate the presence of GFP-positive cells.

solid medium, each cell type was seeded in quadruplicate at a density of 5×10^3 cells in 6-well plates. Cells were mixed with 1.4 ml of 0.3% agar noble in RPMI 1640 plus 10% FCS (MMH-D3, MMH-R, A549) or 15% FCS plus 1 ng/ml TGF-β1 (MMH-RT). The suspension was poured onto a bottom layer of 1.4 ml of 0.7% agar noble in RPMI plus 10% FCS (MMH-D3, MMH-R, A549) or 15% FCS plus 4 ng/ml TGF-β1 (MMH-RT). Growth factors (40 ng/ml TGF-α, 30 ng/ml IGF-II and 1.4 nM insulin) for MMH-D3 and MMH-R cells were immersed at a two-fold concentration in the bottom agar layer. After 14 days, colonies were counted and evaluated statistically. The assay was performed twice for each cell type.

Tumor formation in vivo and recovery of tumor cells

Cells were detached from tissue culture plates by trypsinization, washed with PBS and counted. Aliquots of 1×10^6 MMH-D3, MMH-R or MMH-RT cells were resuspended in 200 μl Ringer solution and subcutaneously injected into immunocompromized SCID/BALB/c recipient mice. Tumor induction was viewed by palpation and the size of tumors was periodically determined using a vernier caliper. The tumor weight was calculated from tumor size using the formula: (diameter×diameter×length/2). 21 to 28 days after cell injection, areas containing tumors were surgically removed and cut into small pieces under sterile conditions using a scalpel. Pieces of tumor tissue were

immediately frozen in liquid nitrogen for further histological analysis. To recover GFP-positive tumor cells for growth in tissue culture, small pieces of tumor tissue were put in culture plates, and attached cells were subcultured at a ratio of 1:3 twice a week in RPMI 1640 supplemented with 15% FCS plus 1 ng/ml TGF-β1. All experiments were performed according to the Austrian guidelines for animal care and protection.

Invasion assay

Invasion assays were performed with 24-well Biocoat Matrigel invasion chambers (Becton Dickinson, Franklin Lakes, USA) according to the instructions of the manufacturer. Briefly, Matrigel inserts were re-hydrated in RPMI plus 10% FCS for 2 hours at room temperature. After aspiration of medium, cells in their respective growth medium (500 µl) were plated at 90% confluency. The lower chamber was filled with 250 µl of conditioned medium obtained from mouse 3T3 fibroblasts. Following 24 and 48 hours of incubation, the Matrigel layer and non-invasive cells were removed with a cotton swab. The filters were fixed in 8% paraformaldehyde/PBS for 30 minutes, removed from the inserts and mounted to detect GFP-positive cells by fluorescence microscopy.

Cell structures in collagen gels

Cells trypsinized from tissue culture plates were washed with PBS and counted. Per collagen gel, 1×10^4 cells were resuspended in 50 µl serum-free mammary epithelial cell growth medium (MECGM; PromoCell, Heidelberg, Germany) and mixed with 1 ml ice-cold collagen solution, containing a mixture of 1-2% rat tail collagen, 1 x MEM-Hanks, 20 mM HEPES, pH 7.4, 0.22% $NaHCO_3$, 0.21% NaOH (Parzefall et al., 1985). The mixtures were put into 24-well plates and allowed to solidify into gels for 30 minutes at 37°C. Subsequently, collagen gels were overlaid with serum-free MECGM containing 40 ng/ml TGF-α, 30 ng/ml IGF-II and 1.4 nM insulin. In some cases, TGF-β1 was added at a concentration of 5 ng/ml (indicated in the text). The medium with respective growth factors was changed every second day.

Enzyme linked immunosorbent assay (ELISA) for TGF-β1

For determination of TGF-β1 secreted into the medium, cells were grown in the following media for 40 hours: MMH and MMH-R cells, RPMI/4% FCS supplemented with TGF-α, IGF-II and insulin; MMH-RT and ex tumor cells, serum-free MECGM plus TGF-α, IGF-II and insulin. ELISAs were performed in triplicate, using the Quantikine® human TGF-β1 immunoassay (R&D Systems, Minneapolis, USA) according to the instructions of the manufacturer. Briefly, aliquots of cell culture supernatants were used either directly or after acidification. Latent TGF-β1 was activated by addition of 100 µl 1 M HCl to 500 µl supernatant. After incubation at room temperature for 10 minutes, the solution was neutralized with 100 µl 0.2 M NaOH and 10 mM HEPES/KOH, pH 7.5. All values were normalized to background measurements from respective growth media and calculated on the basis of a TGF-β1 standard curve.

Cultivation of MMH-R cells in conditioned medium generated by fibroblastoid MMH-RT cells

MMH-RT cells were grown in RPMI 1640 plus 15% FCS or serum-free MECGM. Conditioned media harvested after 40 hours were supplemented with FCS to a final concentration of 20% (total 35%) and TGF-α, IGF-II and insulin was added. For controls, RPMI plus 15% FCS or 40% FCS was treated alike. MMH-R cells at about 50% confluency were grown either in conditioned TGF-β1-activated media or control media for 48 hours.

Reverse transcriptase polymerase chain reaction (RT-PCR)

Poly(A)$^+$-mRNA was extracted and reverse transcribed with a mRNA isolation and first-strand cDNA synthesis kit (Roche, Mannheim, Germany). Aliquots of the resulting products were employed as templates for specific PCR amplifications using Ready-To-Go PCR beads (Amersham Pharmacia Biotech, Uppsala, Sweden). The conditions for PCR reaction were optimized for each primer pair. The following forward and reverse primers were used for specific amplifications: pregnane X receptor (PXR), TGAGACCTGAGGAGAGCTGG and ATGATCTCTTTCCCGTCGCT; E-cadherin, GAGCCTGAGTCCTGCAGTCC and TGTATTGCTGCTTGGCCTCA; desmoplakin, CCGACACGACTCCGTGAGTA and CGAGATCCGGACCTTGAACC; cytokeratin 14 (CK14), AAGATCCTGGCAGCCACCGT and CGGTTGGTGGAGGTCACATC; laminin-alpha5, GCCAGCAAGGTCAAGGTGTC and AACTGATGCCCGTGGTGTTC; albumin, GAGATCGCCCATCGGTATAA and TCTTCTGGCAACTTCATGCA; PAI-1, GTGATGCTTGGCAACCCACG and GGTGGAGACATAACAGATGCAG; fibronectin, CACTGGCTTCCAAGTCGATG and CTTCGTCGGTGCCAACTGGT; CD44, CCTGGCACATCAGCAGATCG and AGATTCCGGGTCTCGTCAGC; matrix metalloproteinase 9 (MMP-9), CGCTCATGTACCCGCTGT and TCACCTCATGGTCCACCTTG; snail, ACCTTCCAGCAGCCCTACGACC and GTGTGGCTTCGGATGTGCATC; rhoA, GTGGAATTCGCCTTGCATCTGAGAAGT and CACGAATTCAATTAACCGCATGAGGCT. The amplification products were subsequently analyzed by electrophoresis on 1.5% agarose gels and staining with ethidium bromide.

Results

Polarized, epithelial Met Murine Hepatocytes (MMH-D3) are sensitive to TGF-β1-mediated growth inhibition

We employed factor-dependent immortalized hepatocytes isolated from transgenic mice expressing a truncated cytoplasmic domain of human c-Met in the liver (Amicone et al., 1995). Importantly, the established cell line used in this study, termed MMH-D3, is non-tumorigenic and has reduced expression of exogenous c-Met to undetectable levels, like other hepatocyte cell lines derived from different developmental stages of the Met transgene (data not shown) (Amicone et al., 1997). These findings led to the idea that cytoplasmic Met was apparently required for the induction rather than the maintenance of immortalization. In addition, these MMH-D3 cells represent a pure population of Met murine hepatocytes, as no other cell types sharing a precursor potential could be identified in this cell line (Spagnoli et al., 1998). Most strikingly, MMH-D3 express albumin and a panel of hepatocyte-enriched transcription factors and hepatic markers, indicating that these hepatocytes maintain their highly differentiated program throughout multiple cell divisions (Amicone et al., 1997). Consistent with these data, we observed that MMH-D3 cells grow in a strictly contact-inhibited manner and display epithelial morphology as observed by the immunostaining pattern of components participating in intercellular communication. We found that the adherens junction molecules E-cadherin and the E-cadherin-associated β-catenin protein localize to cell-cell contacts (Fig. 1A). Moreover, the tight junction component ZO-1 exhibited staining at cell boundaries (Fig. 1A), which was exclusively restricted to the apical end of cells (xz section, data not shown), indicating a polarized cellular phenotype. A similar localization at cell margins was obtained for the catenin family

member p120^{ctn} and desmoplakin, and the latter is known to be a functional constituent of desmosomes (data not shown).

Importantly, treatment of these epithelial MMH-D3 hepatocytes with TGF-β1 resulted in growth inhibition within 72 hours (Fig. 1B) and cells arrested in the G1 phase of the cell cycle (Fig. 1C). Furthermore, long-term treatment (>7 days) of MMH-D3 cells with TGF-β1 lead to cell death. Titration experiments revealed that MMH-D3 cells effectively responded to TGF-β1 at concentrations ranging between 0.5 ng/ml and >30 ng/ml (data not shown). These observations are in clear accordance with previous investigations reporting that TGF-β1 inhibits DNA synthesis in primary hepatocytes which is associated with an increased emergence of apoptotic events (Oberhammer et al., 1991; Oberhammer et al., 1992; Grasl-Kraupp et al., 1998; Spagnoli et al., 1998). From the described data we concluded that MMH-D3 cells consist of a well-defined polarized epithelial cell architecture and are, like normal hepatocytes, susceptible to growth arrest and induction of cell death by TGF-β1.

Polarized, epithelial hepatocytes expressing constitutive active Ha-Ras undergo epithelial to fibroblastoid conversion (EFC) without growth inhibition upon treatment with TGF-β1

Epithelial MMH-D3 cells were retrovirally transmitted with a construct bicistronically expressing constitutive active v-Ha-Ras (Oft et al., 1996; Redmond et al., 1988) and GFP. Linkage of v-Ha-Ras cDNA under control of a virally derived long terminal repeat ensured stable ectopic expression through multiple cell divisions of hepatocytes (Fig. 3B) (Huber and Cordingley, 1988). Interestingly, the proliferation of the resulting cell line (termed MMH-R) was still dependent on the exogenous growth factors TGF-α, IGF-II and insulin, and they again formed monolayers of cells with a polarized epithelial architecture, comparable with the one displayed by the parental MMH-D3 cells (Fig. 2, left panel). Likewise, the immunostaining pattern for the adherens junction components E-cadherin, β-catenin and p120^{ctn} remained restricted to cell-cell boundaries. The localization of ZO-1 and desmoplakin at cell borders was indicative of the presence of intact tight junctions and desmosomes, respectively. Additionally, actin was found to form the typical network of filaments lining cell boundaries, a feature characteristic of epithelial cells. Moreover, the cytoplasmic distribution of the TGF-β-responsive signaling molecule Smad2 suggested its presence in a presumably inactive form, as detected in parental MMH-D3 cells (Fig. 2; data not shown).

However, treatment of MMH-R hepatocytes with TGF-β1 induced a highly synchronous transition from a polarized, epithelial to a depolarized, spindle-shaped and fibroblastoid morphology within 12-24 hours (Fig. 2, right panel). This phenotypic switch rapidly occurred at concentrations ranging from 0.5 ng/ml to >30 ng/ml TGF-β1, irrespective of the attachment of MMH-R cells on plastic or collagen-coated tissue culture plates. In sharp contrast to the growth inhibitory role of TGF-β1 on parental epithelial MMH-D3 cells, TGF-β1-treated fibroblastoid cells were found to loose contact inhibition and to grow in polylayers. Most notably, these cells showed a proliferation kinetics comparable to the one of untreated epithelial MMH-D3 and MMH-R cells (Fig. 3A).

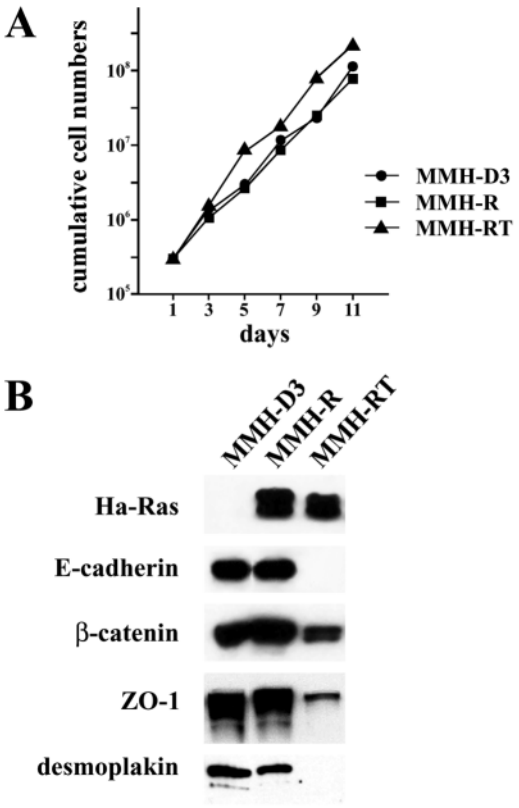

Fig. 3. Cell cycle progression of MMH cell types and expression of marker proteins. (A) Proliferation kinetics of epithelial (MMH-D3, circles; MMH-R, squares) versus fibroblastoid MMH-RT cells (triangles). (B) Protein abundance of representative components participating in intercellular communication in epithelial and fibroblastoid cells. Besides the exogenous expression of Ha-Ras in epithelial MMH-R and fibroblastoid MMH-RT cells, the downregulation and loss of respective markers is indicated in fibroblastoid cells by immunoblotting.

Moreover, fibroblastoid-converted MMH-R cells exhibited factor-independent growth since the proliferation kinetics did not change, irrespective of the supplementation of TGFα, IGF-II and insulin alone or in combination (data not shown). In consequence, these fibroblastoid cells, later on referred to as MMH-RT, were cultured in medium containing fetal calf serum and TGF-β1 without additional growth factors.

In contrast to polarized MMH cell types, fibroblastoid MMH-RT derivatives showed a dramatic change in the expression levels and subcellular distribution of epithelial markers (Fig. 2, right panel). Confocal immunofluorescence microscopy revealed that the tumor suppressor E-cadherin was hardly detectable; it also revealed the cytoplasmic redistribution of β-catenin, p120^{ctn} and ZO-1. Desmoplakin even declined to undetectable levels, and a pronounced stress fiber formation of actin polymers was observed. Furthermore, Smad2 was already exclusively localized in cell nuclei 30 minutes after TGF-β1 induction, indicating TGF-β1-mediated transactivation of the signaling molecule. In accordance with these data, the analysis of protein levels showed a loss of E-cadherin and desmoplakin expression as well as a significant reduction of β-catenin and ZO-1 protein levels in fibroblastoid MMH-RT cells (Fig. 3B). As expected, the transepithelial

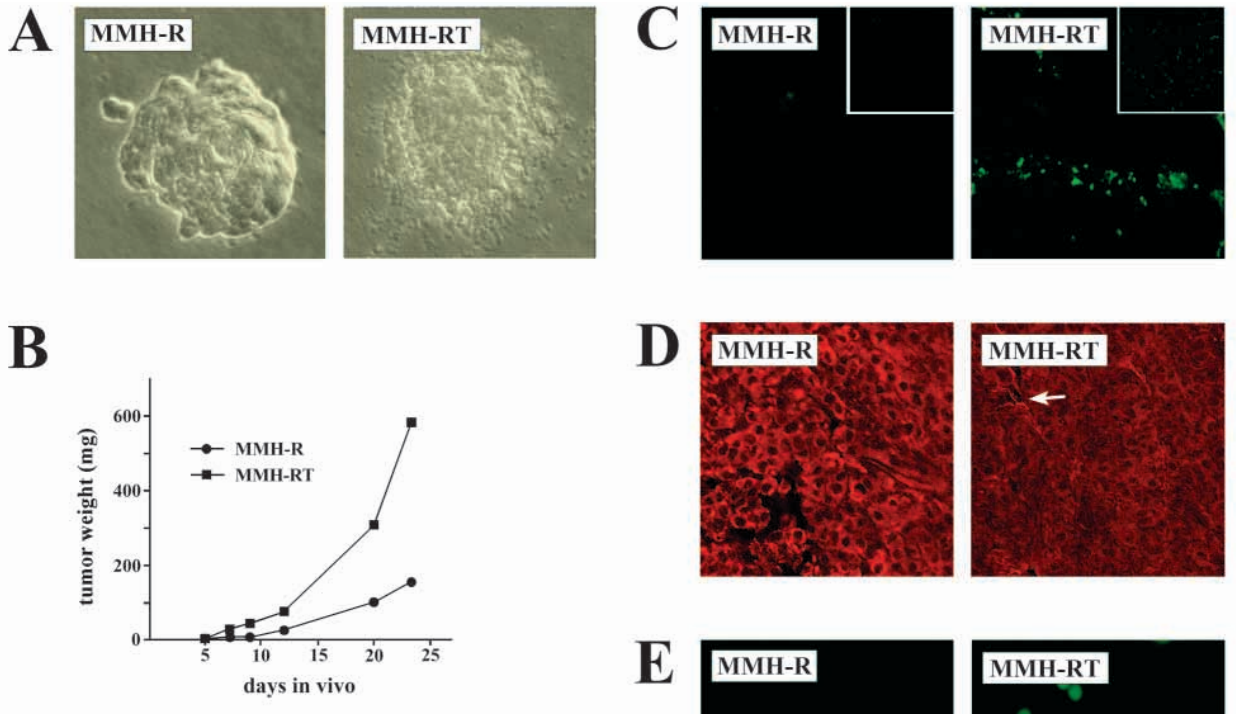

Fig. 4. Malignant transformation of epithelial MMH-R and fibroblastoid MMH-RT cells analyzed in vitro and in vivo. (A) Phase contrast images depicting the typical colonies formed in vitro by anchorage-independent growth of MMH-R and MMH-RT cells in soft agar. (B) Kinetics of tumor formation in vivo after subcutaneous injection of MMH-R (circles) and MMH-RT cells (squares) into immunocompromized SCID/BALB/c recipient mice. (C) Visualization of endothelial cells in histological sections of tumors by immunological staining with anti-von Willebrand Factor. Insets represent lower magnifications (10×) of histological sections. (D) Dedifferentiation of epithelial MMH-R and fibroblastoid MMH-RT cells after tumor formation in vivo. Histological sections of tumors give rise to poorly differentiated cell carcinomas as shown by immunological staining with ZO-1. The cytoplasmic distribution of ZO-1 appears to be very weak in vascularized MMH-RT-derived tumors, and cell boundary staining is exclusively displayed by endothelial cells (white arrow). (E) Assessment of invasive properties in vitro. The ability of epithelial MMH-R and fibroblastoid MMH-RT cells to migrate through Matrigel matrices as reconstituted basement membranes is shown. Invaded cells on lower surfaces of membranes were visualized by immunofluorescence microscopy of GFP-positive MMH-R and MMH-RT cells.

electrical resistance caused by the presence of functional tight junctions, which seal the paracellular spaces between epithelial cells, was completely abolished in layers of depolarized MMH-RT cells (Table 1).

These results indicated that TGF-β1 cooperates with constitutively active Ha-Ras to induce and maintain an EFC of hepatocytes. The process is accompanied by (i) loss of cell adhesion and desmosomal structures, (ii) disruption of the integrity of tight junctions, (iii) drastic changes in the cytoskeletal framework and (iv) nuclear translocation of Smad2. These dramatic alterations pointed to a dedifferentiated phenotype after EFC, and opened the question of the tumorigenic potential of cells at the fibroblastoid stage.

Depolarized, fibroblastoid MMH-RT cells display a highly malignant and invasive phenotype

Transformation-related and tumorigenic properties of epithelial MMH-R versus fibroblastoid MMH-RT cells were analyzed by a broad panel of in vitro and in vivo assays. Both

Table 1. Tumorigenic features of epithelial and fibroblastoid cell types

	MMH-D3	MMH-R	MMH-RT
Phenotype in culture	Epithelial	Epithelial	Fibroblastoid
Transepithelial resistance[a]	+++	++	–
Efficiency of colony formation	$<1\times10^{-3}$	0.2	0.22
Spreading of colonies[b]	–	–	+++
Tumor induction in vivo[c]	–	11-12 days	6-7 days
Vascularization of tumors[d]	–	+/–	+++
Phenotype ex-tumor	–	Fibroblastoid	Fibroblastoid
Invasive growth[e]	–	+/–	+++

[a](+++) >200 Ω×cm^2, (++) 150-200 Ω×cm^2, (–) < 20 Ω×cm^2.

[b](–) no and (+++) vigorous spreading of colonies formed in soft agar (Fig. 4A).

[c]as monitored by initial tumor palpation after subcutaneous injection into SCID/BALB/c mice.

[d](+/–) a small and (+++) a high proportion of endothelial cells in the respective tumor tissue (Fig. 4C).

[e](+/–) a small and (+++) a high number of cells migrate through Matrigel invasion chambers (Fig. 4E).

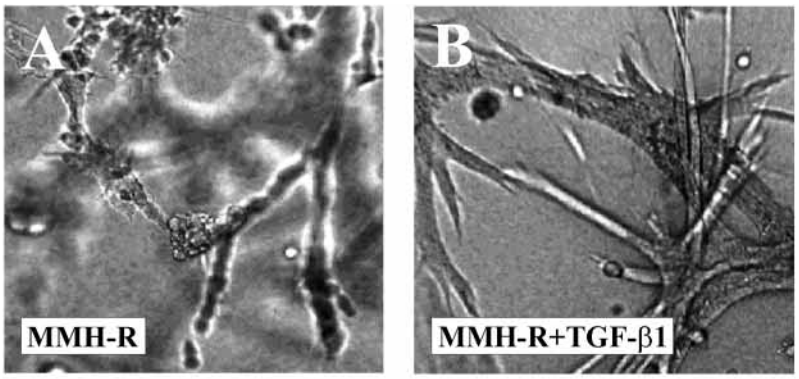

Fig. 5. Typical hepatocellular-derived cell structures in collagen gels. (A) A phase contrast image of epithelial MMH-R cells generating lumen-forming structures. (B) Treatment of epithelial MMH-R cells with exogenous TGF-β1 (5 ng/ml) resulted in the formation of disordered branching cord-like structures.

cell types showed anchorage-independent growth in soft agar assays and formed colonies with a comparable efficiency (about 20%), whereas non-tumorigenic parental MMH-D3 cells were not able to grow under these conditions (Table 1) (Amicone et al., 1997). Contrary to the packed colonies generated by epithelial MMH-R cells, fibroblastoid MMH-RT-derived colonies were diffuse in appearance and exhibited cell spreading, which is indicative of a high motility (Fig. 4A). Interestingly, the highly invasive lung carcinoma cell line A549 yielded dispersed colonies with a similar formation efficiency (data not shown) (Hirai et al., 1991). These data obtained by soft agar assays pointed to a malignant transformation of epithelial MMH-R and fibroblastoid MMH-RT cells; however, depolarized cells additionally displayed the special feature of cell spreading.

Further studies of the ability of MMH-R and MMH-RT cells to generate tumors in vivo revealed yet another difference. Epithelial MMH-R cells produced tumors palpable 11-12 days after subcutaneous injection into immunocompromized SCID/BALB/c recipient mice. However, tumors formed by fibroblastoid MMH-RT were already palpable after 6-7 days (Fig. 4B; Table 1). In addition, fibroblastoid-derived tumors developed an about three-fold higher tumor mass as compared with tumors that originated from epithelial MMH-R cells. These observations, which suggest a more aggressive tumor formation in depolarized MMH-RT cells, were corroborated by the finding that a pronounced vascularization was detectable in fibroblastoid-derived tumors, whereas scarce blood vessel formation was observed in tumors established from epithelial MMH-R cells (Fig. 4C; Table 1). Since large necrotic areas were exclusively localized in MMH-R-derived tumors (data not shown), the proper vascularization might account for the more rapid development of MMH-RT-derived tumors.

Histological analysis revealed that both types of experimental tumors consist of poorly differentiated cells without significant differences in morphology. ZO-1 appeared to be cytoplasmically distributed in sections of both MMH-R- and MMH-RT-derived tumor tissues, indicating a depolarized phenotype of cells in vivo (Fig. 4D). In this regard it is important to note that cells recultivated from both tumors displayed a fibroblastoid morphology pointing to an EFC of MMH-R cells in vivo as well (Table 1). The isolated GFP-positive cell type of MMH-R-derived tumors, termed ex tumor, again exhibited a diffuse cytoplasmic localization of E-cadherin and ZO-1 along with stress fiber formation of actin (data not shown). Hence, this phenotype, which is similar to that of MMH-RT cells generated in vitro, suggests that TGF-β1 might be also a potential candidate to govern hepatocellular EFC in vivo.

By employing Matrigel-coated invasion chambers, we finally observed that fibroblastoid MMH-RT cells show the ability to migrate through Matrigel layers, whereas epithelial MMH-R cells have very restricted behavior in this respect (Fig. 4E; Table 1). Quantitative analysis yielded an about ten-fold higher number of MMH-RT cells with this migratory capacity compared with epithelial MMH-R cells. Taken together, these data indicate that fibroblastoid cells become more malignant and adopt an invasive phenotype after EFC, which accounts for severely vascularized experimental tumors in vivo.

Fibroblastoid MMH-RT cells generate disordered structures in reconstituted collagen gels

The data outlined above were confirmed by using an alternative experimental system, which is thought to mimic more closely the situation in vivo (Oft et al., 1996). For this purpose, cells were cultured in reconstituted collagen matrices in combination with serum-free media in order to monitor hepatocellular EFC under defined conditions. Polarized epithelial cell types developed into lumen-forming structures, which were visible between 7-10 days of cultivation (Fig. 5A). However, upon addition of TGF-β1 to serum-free media overlaying collagen cultures of MMH-R cells, disordered structures of elongated branching cords were observed, again, within 7-10 days of incubation (Fig. 5B). Notably, these disordered structures could be grown into highly dense networks. The observed drastic alterations of cellular plasticity were highly reminiscent of phenotypical changes mediated by Ha-Ras and TGF-β1 on conventional tissue culture plastic. From these results we concluded that the conversion to a fibroblastoid phenotype is the prerequisite for the accumulation of branching cord-like structures, which reflect an invasively growing phenotype in three-dimensional collagen cultures.

Depolarized, fibroblastoid MMH-RT cells establish an autocrine loop of TGF-β1 regulation

As it has been reported that TGF-β1 is highly expressed in hepatocellular carcinomas (Bedossa et al., 1995; Factor et al., 1997; Grasl-Kraupp et al., 1998; Huggett et al., 1991; Ito et al., 1991; Zhao and Zimmermann, 1998), we next asked whether fibroblastoid MMH-RT themselves produce TGF-β1. Thus, we

assayed cell culture supernatants harvested from epithelial and fibroblastoid cell cultures for their respective TGF-β1 content. As described for primary hepatocytes, which synthesize TGF-β in culture, both, MMH-D3 and MMH-R cells, produced low amounts of latent TGF-β1 (Gao et al., 1996). However, we found that fibroblastoid MMH-RT and ex tumor cells secreted about 10-fold higher levels of TGF-β1 into the media than MMH-D3 and MMH-R cells (Fig. 6A). In line with these results, cell culture supernatants obtained from fibroblastoid MMH-RT and ex-tumor cells were on the one hand able to mediate growth inhibition of parental MMH-D3 cells and on the other hand were competent to trigger EFC of MMH-R cells (data not shown). The massive TGF-β1 secretion of fibroblastoid cell types suggests additional functions in the stepwise malignant transformation of hepatocytes. In the initial phase, TGF-β1 induces EFC after cell autonomous Ras activation but at the fibroblastoid stage, TGF-β1 might be necessary to maintain the invasive phenotype.

Loss of E-cadherin is accompanied by upregulation of the transcription factor snail upon hepatocellular EFC

A selective array of genes belonging to diverse functional classes was further analyzed to estimate a potential reprogramming of gene expression upon hepatocellular EFC. By determining steady state mRNA levels from polarized MMH-R versus depolarized MMH-RT cells using RT-PCR, we found that the expression of genes associated with differentiation of hepatocytes like PXR, a putative downstream target of the hepatocyte nuclear factor (HNF)-4α (Li et al., 2000), and albumin were virtually abolished (Fig. 6B). In accordance with the entire collapse of epithelial architecture, the expression of E-cadherin and desmoplakin declined to almost undetectable levels (Fig. 2, Fig. 3B). A similar result was obtained for the intermediate filament component CK14. Laminin A5, representing a ligand of integrins, whose signaling contributes to cell adhesion and the maintenance of a differentiated epithelial phenotype (Kikkawa et al., 1998), was also significantly reduced. In contrast, PAI-1 and fibronectin, previously identified as TGF-β targets, which fulfil crucial functions in the modification of the extracellular matrix (ECM) composition (Ten-Dijke et al., 2000; Hocevar et al., 1999), were strongly upregulated in fibroblastoid MMH-RT cells (Fig. 6B). Moreover, in line with invasiveness of MMH-RT cells, MMP-9 appeared to be exclusively expressed in depolarized cells. Additionally, a significant increase of the hyaluronan receptor CD44 was detected, whose elevated abundance has already been described at later stages of liver carcinomas (Endo and Terada, 2000). Most interestingly with respect to the loss of E-cadherin expression in fibroblastoid cells, a strong accumulation of the zinc finger transcription factor Snail was detectable. This finding is of particular interest, as Snail has been reported to act as a potential regulator that is able to repress the E-cadherin promoter and to govern epithelial to mesenchymal (fibroblastoid) transition on its own (Batlle et al., 2000; Cano et al., 2000). These results suggest that hepatocellular EFC correlates with both functional dedifferentiation and reprogramming of the epithelial gene expression pattern towards an invasive stage, including remodeling of ECM proteins and repression of E-cadherin by Snail.

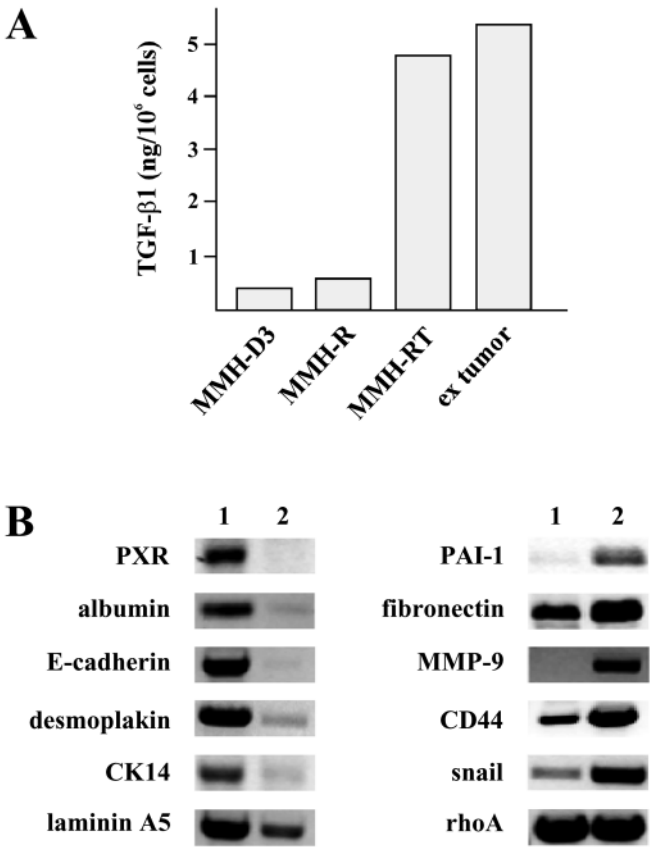

Fig. 6. Molecular characteristics of epithelial MMH-R versus established fibroblastoid MMH-RT cells. (A) TGF-β1 production of epithelial and fibroblastoid cell types. The amount of latent TGF-β1 secretion into the medium was determined by ELISA. (B) Semi-quantitative RT-PCR determining the selective decrease (left panel) and increase (right panel) of mRNA abundance in epithelial versus fibroblastoid cells. All samples contained equal amounts of cDNA. As a control, rhoA mRNA expression remained unaffected (right panel). Lane 1, epithelial MMH-R cells; lane 2, fibroblastoid MMH-RT cells.

Fibroblastoid MMH-RT cells revert to an epithelial-like phenotype through the inactivation of PI3 kinase but not of Mek1/2

In a final set of experiments, we started to analyze the signaling pathways responsible for the maintenance of the fibroblastoid state. Thus, experiments were performed that aimed to revert the fibroblastoid phenotype of long-term growing MMH-RT cells to an epithelial-like morphology within 24 hours, a time period representative of the induction of hepatocellular EFC. Interestingly, inhibition of Mek1/2 activity, which operates downstream of Raf and stimulates Erk, by the low molecular inhibitor UO126, had no effect on the established fibroblastoid cell architecture (Fig. 7A). Similar results were obtained with the Mek1/2 antagonist PD98059 (data not shown), suggesting that signaling through the Mek pathway is not required to maintain the fibroblastoid state. In sharp contrast, the functional inactivation of PI3 kinase signaling by treatment of cells with LY294.002 resulted in a reversion of fibroblastoid MMH-RT to an epithelial-like morphology (Fig. 7A). A similar interference

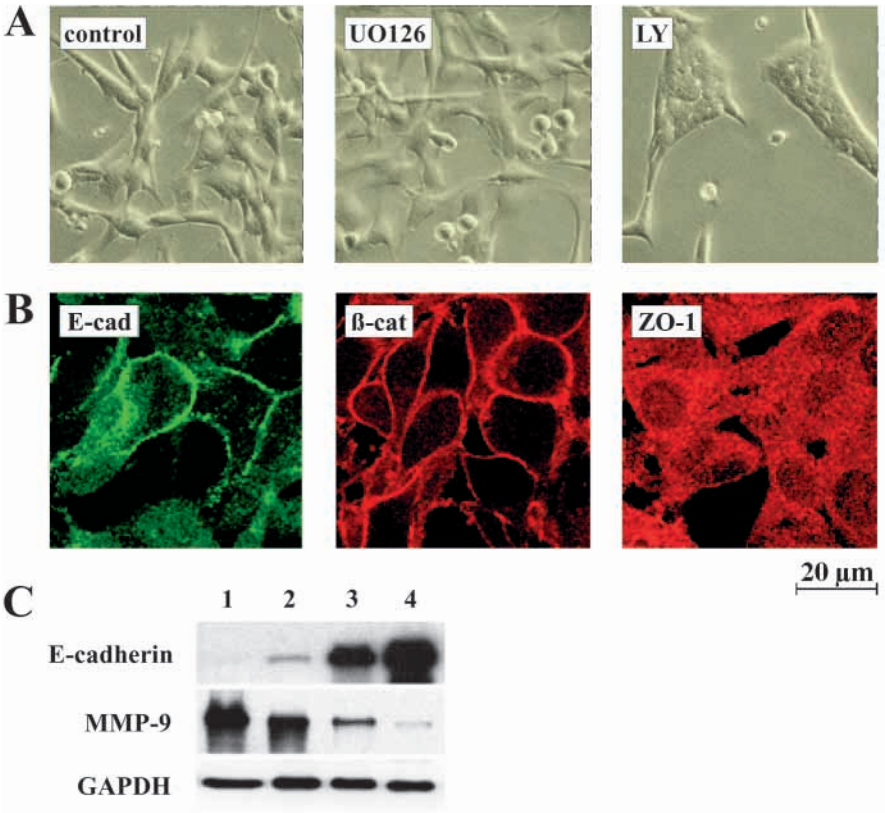

Fig. 7. Reversion of fibroblastoid MMH-RT cells to an epithelium-like phenotype. (A) Phase contrast microscopy of MMH-RT cells (control) grown on tissue culture plates and either treated with 30 µM UO126 or 5 µM LY294.002 for 24 hours. (B) Confocal immunofluorescence microscopy of MMH-RT cells treated with 5 µM LY294.002 for 24 hours. (C) Expression of E-cadherin and MMP-9 as determined by immunoblotting. Staining of glyceraldehyde-3-phosphate dehydrogenase (GAPDH) is shown as a loading control. Lane 1, fibroblastoid MMH-RT cells; lanes 2 and 3, MMH-RT cells treated with 5 µM LY294.002 for 24 and 72 hours, respectively; lane 4, epithelial MMH-R cells.

with PI3 kinase activity through the use of wortmannin as an inhibitory component verified the data achieved with LY294.002 (data not shown). Phenotypic analysis further revealed that this reversion to an epithelium-like one was accompanied by the relocalization of E-cadherin and its associated protein β-catenin on cell margins, whereas ZO-1 still displayed a cytoplasmic distribution (Fig. 7B). The reconversion was further indicated by an increasing re-expression of the tumor suppressor E-cadherin as well as by the reduction of MMP-9 protein levels (Fig. 7C). After prolonged treatment of fibroblastoid cells with LY294.002, E-cadherin and MMP-9 showed expression levels almost comparable with those observed in epithelial MMH-R cells. These data suggest that the inactivation of PI3 kinase in fibroblastoid cells provides epithelial reorganization, which points to a key function of this signal transducer in maintaining the fibroblastoid state. Moreover, the reversion appears as a hierarchical reconstruction of intercellular complexes with a delayed repolarization of cells, as adherens junctions were fully restored at times when tight junctions were still disintegrated.

Discussion

In the current investigation we present direct evidence that TGF-β1 is able to act bifunctionally in hepatocytes: we show that TGF-β1 (i) induces growth arrest and cell death of immortalized hepatocytes and (ii) governs the transition of polarized, epithelial hepatocytes to a spindle-shaped, fibroblastoid phenotype in cooperation with constitutive activate Ha-Ras. The phenotypic switch, termed hepatocellular epithelial to fibroblastoid conversion (EFC), is accompanied by a complete loss of epithelial polarity through dissociation of intercellular contacts and cytoskeletal rearrangements and by the acquisition of an invasive phenotype leading to highly vascularized experimental tumors in vivo. In addition, depolarized fibroblastoid derivatives themselves secrete TGF-β1, suggesting an autocrine regulation of TGF-β signaling necessary to stabilize an invasive hepatocellular phenotype. Finally, we demonstrate that the interference with PI3 kinase through its functional inactivation is sufficient to revert established fibroblastoid cells to an epithelial-like morphology, which points to the important contribution of this signal transducer to the maintenance of hepatocellular EFC.

Hepatocellular EFC: the impact of Ha-Ras and TGF-β1

TGF-β has conflicting roles, with both an anti-proliferative and a tumor-promoting effect. The functional role of TGF-β in liver and other normal epithelial tissues is widely accepted to be an anti-proliferative one. As observed in our model system employing well differentiated, immortalized MMH-D3 (Amicone et al., 1997), TGF-β1 is quite effective at accomplishing this tumor-suppressive task. Treatment of growing MMH-D3 cells with TGF-β1 results in an arrest of proliferation, followed by cell death. Interestingly, TGF-β1-treated MMH-D3 hepatocytes acquired a fibroblastoid morphology before undergoing cell death, which is associated with a breakdown of intercellular complexes at final stages (data not shown). This observation suggests that TGF-β1 is not only a mediator of anti-proliferative events but it also causes drastic alterations in the epithelial organization of hepatocytes.

Similar TGF-β1-induced changes in morphology and polarity were also observed in mammary epithelial cells protected from apoptosis by Bcl-2 (E. Janda and H.B., unpublished). Likewise, these morphogenetic changes are obvious in cooperation with oncogenic activated Ha-Ras. However, these cells show unaffected proliferation kinetics and develop to a more malignant and invasive phenotype under these conditions. From that point of view, TGF-β1 activity can be considered as an executor of hepatocellular fibroblastoid conversion, and activated Ha-Ras signaling is the major source providing the tumorigenic potential. This interpretation is corroborated by the fact that constitutive Ras activation on its own leads to non-invasive malignant transformation (Fig. 4; Table 1), which hardly affects epithelial polarity (Fig. 2). Yet, at the time when Ha-Ras is activated in combination with TGF-β1 stimulation, both signals act synergistically to adopt an invasive phenotype. The latter aspects give a clear-cut rationale for the potential of TGF-β1 to provide a tumor-promoting function, while Ha-Ras can do more than conferring resistance to the growth inhibitory and proapoptotic effects of TGF-β1 (Huggett et al., 1991; Houck et al., 1989).

Interestingly, hepatocyte growth factor (HGF), fibroblast growth factor (FGF)-1 and FGF-2 failed to trigger EFC of MMH-R cells (data not shown), although ligand activation of respective cognate receptors has been suggested to induce scattering of cells in various experimental settings, a process closely related to epithelial to mesenchymal (fibroblastoid) transitions (Boyer et al., 2000). The reason for the lack of induction of EFC, however, might be that the stimulation of HGF or FGF receptors again results in activation of Ras, without affecting pathways contributing to morphogenesis. With this in mind, hyperactivation of Ras appears to be the prerequisite for hepatocellular EFC rather than a trigger on its own.

PI3 kinase probably plays a key role in the maintenance of the fibroblastoid state, as its inhibition results in a reversion to an epithelial-like phenotype (Fig. 7). A similar finding on the crucial role of PI3 kinase has been reported in the TGF-β-mediated mesenchymal transition of murine NMuMG mammary epithelial cells (Bakin et al., 2000). An indication of the significance of PI3 kinase signaling in hepatocellular EFC was seen by the detection of phosphorylation of its downstream target PKB/Akt in fibroblastoid MMH-RT cells, which could also be detected in epithelial MMH-R cells (data not shown). In contrast, deactivation of Erk1/2 through inhibition of Mek1/2 failed to revert fibroblastoid cells, which is in line with the observation that phosphorylation of Erk1/2 could be detected in epithelial MMH-R cells; however, it was hardly present in established MMH-RT cells (J.G. and W.M., unpublished). Similar low levels of activated Erk1/2 were observed in parental MMH-D3 cells. Importantly, these data argue on the one hand for an essential role of the putatively unperturbed Ras/PI3 kinase pathway in sustaining the dedifferentiated state (obviously through its role in cell survival) and on the other hand, Erk1/2 activity appears to be crucial to induce hepatocellular EFC.

Stimulation of TGF-β signaling causes a rapid shift of Smad2 from a diffuse cellular distribution in epithelial MMH-R cells to a nuclear localization in fibroblastoid MMH-RT cells (Fig. 2). Similarly, nuclear Smad2 localization was recently observed in human HCCs (Matsuzaki et al., 2000). So far, these data support the idea that Smad2 might be activated to modulate gene expression in complex with common Smad4; the latter component was recently reported to be constitutively expressed in MMH cell types (Spagnoli et al., 2000). Future work will have to concentrate on the respective roles of Smad signaling and Ras-downstream pathways crosstalking to these TβR-dependent pathways in order to better understand the highly synergistic but also extremely complex interplay between Ha-Ras and TGF-β1 in promoting late events of hepatic tumorigenesis.

Hepatocellular EFC and late stage tumor progression

Our model system mimics the progression of malignant cell transformation towards an invasive phenotype and suggests for the first time that EFC of hepatocytes might be a relevant phenomenon upon hepatocarcinogenesis. This idea is strongly supported by the experimental observations that fibroblastoid MMH-RT cells (i) lose intercellular contacts and respective proteins characteristic of polarized epithelial cells, (ii) show strong modifications of the cytoskeletal framework, (iii) display cell spreading in semisolid soft agar, (iv) generate severely vascularized experimental tumors in vivo, and finally and (v) migrate through reconstituted basement membranes in vitro (Figs 2, 4; Table 1). In sharp contrast, the Ras-transformed but polarized MMH-R cells are restricted with respect to these properties, although their tumorigenesis in the animal is preceded by EFC, presumably owing to TGF-β secreted by mesenchymal cells surrounding the injected MMH-R cells. This synergistic action of Ha-Ras and TGF-β1 causing a shift to a fibroblastoid state in vitro and during tumorigenesis in vivo has been described in other epithelial lineages, that is keratinocytes (Cui et al., 1996; Portella et al., 1998), prostate epithelial (Park et al., 2000) and mammary gland epithelial cells (Oft et al., 1996; Oft et al., 1998; Somasiri et al., 2000; Piek et al., 1999). Consistent with our data, downregulation of the tumor suppressor E-cadherin has been reported to occur frequently in human HCCs and, moreover, has been suggested to be necessary for intrahepatic metastasis (Matsumara et al., 2001; Osada et al., 1996; Slagle et al., 1993). Similarly, the inactivation of E-cadherin-associated β-catenin along with a nuclear accumulation was found in a high percentage of mouse and human HCCs (Terris et al., 1999) as well as in the mesenchymal (fibroblastoid) transition of mammary epithelial cells (Eger et al., 2000). Since EFC-like events were closely correlated with late stage carcinogenesis in several mouse models and owing to the respective observations in human HCCs, it is tempting to speculate that hepatocellular EFC might be a critical event in late liver tumorigenesis.

Establishment of an autocrine loop of TGF-β1 regulation

Interactions between the epithelium and the mesenchyme clearly involves soluble factors acting in a paracrine manner to transmit specific information (Birchmeier et al., 1995; Birchmeier and Birchmeier, 1993). In the liver, the non-parenchymal compartment has been described as the major source for TGF-β1, whereas hepatocytes in the parenchyma fail to express detectable levels of this cytokine (Rossmanith and Schulte-Hermann, 2001). Thus, the mito-inhibitory

function of TGF-β on normal hepatocytes has been suggested to arise from a paracrine mode of regulation. By contrast, as shown by several reports, abundant TGF-β levels are detectable in HCCs accompanied by a malignant progression (Bedossa et al., 1995) and, furthermore, elevated TGF-β concentrations could be measured in the serum of HCC patients (Shirai et al., 1994). The first light to be shed on this obvious discrepancy was by recent studies demonstrating that TGF-β1 constitutively activates Smad2 in an autocrine fashion in human HCCs (Matsuzaki et al., 2000). Interestingly, the data provided by the current study clearly confirm this finding, as TGF-β1 secretion was highly increased in fibroblastoid MMH-RT cells and cell culture supernatants of these cells were able to induce EFC of MMH-R cells along with a stimulation of nuclear Smad2 localization. Our data provide further evidence that a switch from a paracrine to an autocrine regulation of TGF-β signaling occurs, which might be important for the late steps in hepatocarcinogenesis. However, the switch in the regulatory loop leading to an autocrine stimulatory mechanism, which is above sub-threshold levels of TGF-β1 production, appears to depend on the activation of Ras. In synergy with Ras, the autocrine regulation of TGF-β signaling has on the one hand the potential to recruit epithelial MMH-R cells to undergo EFC, and on the other hand to the potential to maintain the fibroblastoid, invasive state.

Reprogramming of gene expression upon hepatocellular EFC

Not surprisingly, the induction of hepatocellular EFC depends on de novo RNA and protein synthesis, as inhibition of transcription and translation by the treatment of MMH-R cells with actinomycin D and cycloheximide, respectively, prevented the TGF-β1-mediated fibroblastoid conversion (data not shown). These observations motivated us to analyze changes in the steady state transcript levels of a selective panel of genes in epithelial versus fibroblastoid cells (>30 genes in total). The results obtained clearly indicate that hepatocellular EFC is accompanied by an epithelial dedifferentiation process as the expression of albumin, PXR, E-cadherin and desmoplakin is abolished in fibroblastoid cells (Fig. 6B). In addition, the increased expression of PAI-1, fibronectin and MMP-9 strongly suggest that MMH-RT cells have acquired a stage capable of remodeling and degrading the ECM, as has been described for various types of tumor tissues at late stages of malignant progression. A potential regulatory candidate responsible for promoting hepatocellular EFC might yet be identified through studies on Snail. This transcription factor is able to bind directly as a repressor to the E-cadherin promoter, and when overexpressed, it has been reported to induce epithelial cells to transform into an invasive, fibroblastoid phenotype on its own (Batlle et al., 2000; Cano et al., 2000). In accordance with these studies, the loss of the tumor suppressor E-cadherin inversely correlated with the upregulation of Snail upon hepatocellular EFC. So far, however, Snail-mediated alterations could not be detected in experiments aimed at ectopically expressing Snail in MMH-D3 and MMH-R cells, most probably owing to the low level of exogenous Snail expression (data not shown). Further investigations will focus on the regulatory role of Snail upon EFC and will elucidate whether Snail represents a potential marker for HCCs.

A promising future prospect is the study of the sequence of molecular events following TGF-β1-induced progression of Ras-hepatocytes (MMH-R) towards an increased malignant and invasive phenotype. Importantly, the described hepatocellular EFC occurs highly synchronously on simple tissue culture plastic without requiring more complex conditions. This makes the described tumor model system an ideal tool for high-throughput approaches in order to analyze alterations at the level of gene expression between cell populations simultaneously passing the steps towards establishing the fibroblastoid state. We expect that such kinetic analyses of gene expression profiles during EFC will help to dissect the molecular mechanisms responsible for late malignant events of hepatocytes. In this respect, (de)activation of gene products contributing to vascularization are of potential interest. The proposed detailed analysis at the molecular level and the comparison of results with observations made in human HCCs will clarify the relevance of this murine tumor model for investigation of human hepatocarcinogenesis. The identification of signaling pathways contributing to hepatocellular EFC may help to identify new targets for therapeutical intervention at late steps in hepatocarcinogenesis, such as PI3 kinase or up/downstream signal transducers.

The authors thank Marco Tripodi, Universita La Sapienza, Italy, for providing MMH-D3 cells and David R. Garrod, University of Manchester, UK for anti-desmoplakin antibody. We also want to express our appreciation to Daniela Schaferl for excellent technical assistance and to Alexandra Fischer and Mario Mikula for helpful discussions and critical reading of the manuscript. This work was supported by the 'Hochschuljubiläumsstiftung der Stadt Wien', Austria and by grants from the Institute of Cancer Research, Vienna.

References

Amicone, L., Galimi, M. A., Spagnoli, F. M., Tommasini, C., De-Luca, V. and Tripodi, M. (1995). Temporal and tissue-specific expression of the MET ORF driven by the complete transcriptional unit of human A1AT gene in transgenic mice. *Gene* **162**, 323-328.

Amicone, L., Spagnoli, F. M., Spath, G., Giordano, S., Tommasini, C., Bernardini, S., De-Luca, V., Della-Rocca, C., Weiss, M. C., Comoglio, P. M. and Tripodi, M. (1997). Transgenic expression in the liver of truncated Met blocks apoptosis and permits immortalization of hepatocytes. *EMBO J.* **16**, 495-503.

Bakin, A. V., Tomlinson, A. K., Bhowmick, N. A., Moses, H. L. and Arteaga, C. L. (2000). Phosphatidylinositol 3-kinase function is required for transforming growth factor beta-mediated epithelial to mesenchymal transition and cell migration. *J. Biol. Chem.* **275**, 36803-36810.

Batlle, E., Sancho, E., Franci, C., Dominguez, D., Monfar, M., Baulida, J. and Garcia-De-Herreros, A. (2000). The transcription factor snail is a repressor of E-cadherin gene expression in epithelial tumour cells. *Nat. Cell. Biol.* **2**, 84-89.

Bedossa, P., Peltier, E., Terris, B., Franco, D. and Poynard T. (1995). Transforming growth factor-beta 1 (TGF-beta 1) and TGF-beta 1 receptors in normal, cirrhotic, and neoplastic human livers. *Hepatology* **21**, 760-766.

Birchmeier, C. and Birchmeier, W. (1993). Molecular aspects of mesenchymal-epithelial interactions. *Annu. Rev. Cell Biol.* **9**, 511-540.

Birchmeier, C., Meyer, D. and Riethmacher, D. (1995). Factors controlling growth, motility, and morphogenesis of normal and malignant epithelial cells. *Int. Rev. Cytol*. **160**, 221-266.

Bos, J. L. (1989). Ras oncogenes in human cancer: a review. *Cancer Res.* **49**, 4682-4689.

Boyer, B., Valles, A. M. and Edme, N. (2000). Induction and regulation of epithelial-mesenchymal transitions. *Biochem. Pharmacol.* **60**, 1091-1099.

Cano, A., Perez-Moreno, M. A., Rodrigo, I., Locascio, A., Blanco, M. J., del-Barrio, M.G., Portillo, F. and Nieto, M. A. (2000). The transcription factor snail controls epithelial-mesenchymal transitions by repressing E-cadherin expression. *Nat. Cell. Biol.* **2**, 76-83.

Clark, G. J. and Der, C. J. (1995). Aberrant function of the Ras signal transduction pathway in human breast cancer. *Breast Cancer Res. Treat.* **35**, 133-144.

Cui, W., Fowlis, D. J., Bryson, S., Duffie, E., Ireland, H., Balmain, A. and Akhurst, R. J. (1996). TGFbeta1 inhibits the formation of benign skin tumors, but enhances progression to invasive spindle carcinomas in transgenic mice. *Cell* **86**, 531-542.

Downward, J. (1998). Ras signalling and apoptosis. *Curr. Opin. Genet. Dev.* **8**, 49-54.

Eger, A., Stockinger, A., Schaffhauser, B., Beug, H. and Foisner, R. (2000). Epithelial mesenchymal transition by c-Fos estrogen receptor activation involves nuclear translocation of beta-catenin and upregulation of beta-catenin/lymphoid enhancer binding factor-1 transcriptional activity. *J. Cell Biol.* **148**, 173-188.

Endo, K. and Terada, T. (2000). Protein expression of CD44 (standard and variant isoforms) in hepatocellular carcinoma: relationships with tumor grade, clinicopathologic parameters, p53 expression, and patient survival. *J. Hepatol.* **32**, 78-84.

Factor, V. M., Kao, C. Y., Santoni-Rugiu, E., Woitach, J. T., Jensen, M. R. and Thorgeirsson, S. S. (1997). Constitutive expression of mature transforming growth factor beta1 in the liver accelerates hepatocarcinogenesis in transgenic mice. *Cancer Res.* **57**, 2089-2095.

Fausto, N. and Webber, E. M. (1993). Control of liver growth. *Crit. Rev. Eukaryot. Gene Expr.* **3**, 1117-1135.

Fausto, N. (2000). Liver regeneration. *J. Hepatol.* **32**, 19-31.

Gao, C., Gressner, G., Zoremba, M. and Gressner, A. M. (1996). Transforming growth factor beta (TGF-beta) expression in isolated and cultured rat hepatocytes. *J. Cell. Physiol.* **167**, 394-405.

Gotzmann, J., Eger, A., Meissner, M., Grimm, R., Gerner, C., Sauermann, G. and Foisner R. (1997). Two-dimensional electrophoresis reveals a nuclear matrix-associated nucleolin complex of basic isoelectric point. *Electrophoresis* **18**, 2645-2653.

Grasl-Kraupp, B., Rossmanith, W., Ruttkay-Nedecky, B., Mullauer, L., Kammerer, B., Bursch, W. and Schulte-Hermann, R. (1998). Levels of transforming growth factor beta and transforming growth factor beta receptors in rat liver during growth, regression by apoptosis and neoplasia. *Hepatology* **28**, 717-726.

Graziani, A., Gramaglia, D., dalla-Zonca, P. and Comoglio, P. M. (1993). Hepatocyte growth factor/scatter factor stimulates the Ras-guanine nucleotide exchanger. *J. Biol. Chem.* **268**, 9165-9168.

Hanahan, D. and Weinberg, R. A. (2000). The hallmarks of cancer. *Cell* **100**, 57-70.

Hay, E. D. (1990). Epithelial-mesenchymal transitions. *Semin. Dev. Biol.* **1**, 347-356.

Hirai, K., Shimada, H., Ogawa, T. and Taji, S. (1991). The spread of human lung cancer cells on collagens and its inhibition by type III collagen. *Clin. Exp. Metastasis* **9**, 517-527.

Hocevar, B. A., Brown, T. L. and Howe, P. H. (1999). TGF-beta induces fibronectin synthesis through a c-Jun N-terminal kinase-dependent, Smad4-independent pathway. *EMBO J.* **18**, 1345-1356.

Houck, K. A., Michalopoulos, G. K. and Strom, S. C. (1989). Introduction of a Ha-ras oncogene into rat liver epithelial cells and parenchymal hepatocytes confers resistance to the growth inhibitory effects of TGF-beta. *Oncogene* **4**, 19-25.

Huber, B. E. and Cordingley, M. G. (1988). Expression and phenotypic alterations caused by an inducible transforming ras oncogene introduced into rat liver epithelial cells. *Oncogene* **3**, 245-256.

Huggett, A. C., Ellis, P. A., Ford, C. P., Hampton, L. L., Rimoldi, D. and Thorgeirsson, S. S. (1991). Development of resistance to the growth inhibitory effects of transforming growth factor beta 1 during the spontaneous transformation of rat liver epithelial cells. *Cancer Res.* **51**, 5929-5936.

Iglesias, M., Frontelo, P., Gamallo, C. and Quintanilla, M. (2000). Blockade of Smad4 in transformed keratinocytes containing a Ras oncogene leads to hyperactivation of the Ras-dependent Erk signalling pathway associated with progression to undifferentiated carcinomas. *Oncogene* **19**, 4134-4145.

Ito, N., Kawata, S., Tamura, S., Takaishi, K., Shirai, Y., Kiso, S., Yabuuchi, I., Matsuda, Y., Nishioka, M. and Tarui, S. (1991). Elevated levels of transforming growth factor beta messenger RNA and its polypeptide in human hepatocellular carcinoma. *Cancer Res.* **51**, 4080-4083.

Jo, M., Stolz, D. B., Esplen, J. E., Dorko, K., Michalopoulos, G. K. and Strom, S. C. (2000). Cross-talk between epidermal growth factor receptor and c-Met signal pathways in transformed cells. *J. Biol. Chem.* **275**, 8806-8811.

Kikkawa, Y., Sanzen, N. and Sekiguchi, K. (1998). Isolation and characterization of laminin-10/11 secreted by human lung carcinoma cells. laminin-10/11 mediates cell adhesion through integrin alpha3 beta1. *J. Biol. Chem.* **273**, 15854-15859.

Li, J., Ning, G. and Duncan, S. A. (2000). Mammalian hepatocyte differentiation requires the transcription factor HNF-4alpha. *Genes Dev.* **14**, 464-474.

Markowitz, S., Wang, J., Myeroff, L., Parsons, R., Sun, L., Lutterbaugh, J., Fan, R. S., Zborowska, E., Kinzler, K. W., Vogelstein, B., Brattain, M. and Wilson, J. K. V. (1995). Inactivation of the type II TGF-beta receptor in colon cancer cells with microsatellite instability. *Science* **268**, 1336-1338.

Massague, J. (1990). The transforming growth factor-beta family. *Annu. Rev. Cell. Biol.* **6**, 597-641.

Massague, J. and Chen, Y. G. (2000). Controlling TGF-beta signaling. *Genes Dev.* **14**, 627-644.

Matsumura, T., Makino, R. and Mitamura, K. (2001). Frequent down-regulation of E-cadherin by genetic and epigenetic changes in the malignant progression of hepatocellular carcinomas. *Clin. Cancer Res.* **7**, 594-599.

Matsuzaki, K., Date, M., Furukawa, F., Tahashi, Y., Matsushita, M., Sakitani, K., Yamashiki, N., Seki, T., Saito, H., Nishizawa, M., Fujisawa, J. and Inoue, K. (2000). Autocrine stimulatory mechanism by transforming growth factor beta in human hepatocellular carcinoma. *Cancer Res.* **60**, 1394-1402.

McCormick, F. (1999). Signalling networks that cause cancer. *Trends Cell. Biol.* **9**, M53-56.

Michalopoulos, G. K. and DeFrances, M. C. (1997). Liver regeneration. *Science* **276**, 60-66.

Oberhammer, F., Bursch, W., Parzefall, W., Breit, P., Erber, E., Stadler, M. and Schulte-Hermann, R. (1991). Effect of transforming growth factor beta on cell death of cultured rat hepatocytes. *Cancer Res.* **51**, 2478-2485.

Oberhammer, F. A., Pavelka, M., Sharma, S., Tiefenbacher, R., Purchio, A. F., Bursch, W. and Schulte-Hermann, R. (1992). Induction of apoptosis in cultured hepatocytes and in regressing liver by transforming growth factor beta 1. *Proc. Natl. Acad. Sci. USA* **89**, 5408-5412.

Oft, M., Peli, J., Rudaz, C., Schwarz, H., Beug, H. and Reichmann, E. (1996). TGF-beta1 and Ha-Ras collaborate in modulating the phenotypic plasticity and invasiveness of epithelial tumor cells. *Genes Dev.* **10**, 2462-2477.

Oft, M., Heider, K. H. and Beug, H. (1998). TGFbeta signaling is necessary for carcinoma cell invasiveness and metastasis. *Curr. Biol.* **8**, 1243-1252.

Osada, T., Sakamoto, M., Ino, Y., Iwamatsu, A., Matsuno, Y., Muto, T. and Hirohashi, S. (1996). E-cadherin is involved in the intrahepatic metastasis of hepatocellular carcinoma. *Hepatology* **24**, 1460-1467.

Park, B. J., Park, J. I., Byun, D. S., Park, J. H. and Chi, S. G. (2000). Mitogenic conversion of transforming growth factor-beta1 effect by oncogenic Ha-Ras-induced activation of the mitogen-activated protein kinase signaling pathway in human prostate cancer. *Cancer Res.* **60**, 3031-3038.

Parrish, E. P., Steart, P. V., Garrod, D. R. and Weller, R. O. (1987). Antidesmosomal monoclonal antibody in the diagnosis of intracranial tumours. *J. Pathol.* **153**, 265-273.

Parzefall, W., Galle, P. R. and Schulte-Hermann, R. (1985). Effect of calf and rat serum on the induction of DNA synthesis and mitosis in primary cultures of adult rat hepatocytes by cyproterone acetate and epidermal growth factor. *In Vitro Cell. Dev. Biol.* **21**, 665-673.

Piek, E., Moustakas, A., Kurisaki, A., Heldin, C.-H. and tenDijke, P. (1999). TGF-β type I receptor/ALK-5 and Smad proteins mediate epithelial to mesenchymal transdifferentiation in NMuMG breast epithelial cells. *J. Cell Sci.* **112**, 4557-4568.

Portella, G., Cumming, S. A., Liddell, J., Cui, W., Ireland, H., Akhurst, R. J. and Balmain, A. (1998). Transforming growth factor beta is essential for spindle cell conversion of mouse skin carcinoma in vivo: implications for tumor invasion. *Cell Growth Differ.* **9**, 393-404.

Redmond, S. M., Reichmann, E., Muller, R. G., Friis, R. R., Groner, B. and Hynes, N. E. (1988). The transformation of primary and established mouse mammary epithelial cells by p21-ras is concentration dependent. *Oncogene* **2**, 259-265.

Reynisdottir, I., Polyak, K., Iavarone, A. and Massague, J. (1995). Kip/Cip and Ink4 Cdk inhibitors cooperate to induce cell cycle arrest in response to TGF-beta. *Genes Dev.* **9**, 1831-1845.

Reynolds, S. H., Stowers, S. J., Maronpot, R. R., Anderson, M. W. and Aaronson, S. A. (1986). Detection and identification of activated oncogenes

in spontaneously occurring benign and malignant hepatocellular tumors of the B6C3F1 mouse. *Proc. Natl. Acad. Sci. USA* **83**, 33-37.

Reynolds, S. H., Stowers, S. J., Patterson, R. M., Maronpot, R. R., Aaronson, S. A. and Anderson, M. W. (1987). Activated oncogenes in B6C3F1 mouse liver tumors: implications for risk assessment. *Science* **237**, 1309-1316.

Rommel, C. and Hafen, E. (1998). Ras – a versatile cellular switch. *Curr. Opin. Genet. Dev.* **8**, 412-418.

Rossmanith, W. and Schulte-Hermann, R. (2001). Biology of transforming growth factor β in hepatocarcinogenesis. *Microscopy Res. Technique* **52**, 430-436.

Saitoh, A., Kimura, M., Takahashi, R., Yokoyama, M., Nomura, T., Izawa, M., Sekiya, T., Nishimura, S. and Katsuki, M. (1990). Most tumors in transgenic mice with human c-Ha-ras gene contained somatically activated transgenes. *Oncogene* **5**, 1195-1200.

Sandgren, E. P., Quaife, C. J., Pinkert, C. A., Palmiter, R. D. and Brinster, R. L. (1989). Oncogene-induced liver neoplasia in transgenic mice. *Oncogene* **4**, 715-724.

Schmitz, A. A., Govek, E. E., Bottner, B. and Van Aelst, L. (2000). Rho GTPases: signaling, migration, and invasion. *Exp. Cell Res.* **261**, 1-12.

Shields, J. M., Pruitt, K., McFall, A., Shaub, A. and Der, C. J. (2000). Understanding Ras: 'it ain't over 'til it's over'. *Trends Cell Biol.* **10**, 147-154.

Shirai, Y., Kawata, S., Tamura, S., Ito, N., Tsushima, H., Takaishi, K., Kiso, S. and Matsuzawa, Y. (1994). Plasma transforming growth factor-beta 1 in patients with hepatocellular carcinoma. Comparison with chronic liver diseases. *Cancer* **73**, 2275-2279.

Slagle, B. L., Zhou, Y. Z., Birchmeier, W. and Scorsone, K. A. (1993). Deletion of the E-cadherin gene in hepatitis B virus-positive Chinese hepatocellular carcinomas. *Hepatology* **18**, 757-762.

Somasiri, A., Howarth, A., Goswami, D., Dedhar, S. and Roskelley C.D. (2000). Overexpression of the integrin-linked kinase mesenchymally transforms mammary epithelial cells. *J. Cell Sci.* **114**, 1125-1136.

Spagnoli, F. M., Amicone, L., Tripodi, M. and Weiss, M. C. (1998). Identification of a bipotential precursor cell in hepatic cell lines derived from transgenic mice expressing cyto-Met in the liver. *J. Cell Biol.* **143**, 1101-1112.

Spagnoli, F. M., Cicchini, C., Tripodi, M. and Weiss, M. C. (2000). Inhibition of MMH (Met murine hepatocyte) cell differentiation by TGFbeta is abrogated by pre-treatment with the heritable differentiation effector FGF-1. *J. Cell. Sci.* **113**, 3639-3647.

Strom, S. C. and Faust, J. B. (1990). Oncogene activation and hepatocarcinogenesis. *Pathobiology* **58**, 153-167.

Ten-Dijke, P., Miyazono, K. and Heldin, C. H. (2000). Signaling inputs converge on nuclear effectors in TGF-beta signaling. *Trends Biochem. Sci.* **25**, 64-70.

Terris, B., Pineau, P., Bregeaud, L., Valla, D., Belghiti, J., Tiollais, P., Degott, C. and Dejean, A. (1999). Close correlation between beta-catenin gene alterations and nuclear accumulation of the protein in human hepatocellular carcinomas. *Oncogene* **18**, 6583-6588.

Thiery, J. P. and Chopin, D. (1999). Epithelial cell plasticity in development and tumor progression. *Cancer Metastasis Rev.* **18**, 31-42

Zhao, M. and Zimmermann, A. (1998). Liver cell dysplasia: reactivities for c-met protein, Rb protein, E-cadherin and transforming growth factor-beta 1 in comparison with hepatocellular carcinoma. *Histol. Histopathol.* **13**, 657-670.